Molecular and Crystal Structure of the Anhydrous Form of Chitosan

Toshifumi Yui* and Kiyohisa Imada

Department of Materials Science, Miyazaki University, Miyazaki, 889-21 Japan

Kenji Okuyama, Yutaka Obata, and Katsumi Suzuki

Faculty of Technology, Tokyo University of Agriculture and Technology, Koganei, Tokyo, 184 Japan

Kozo Ogawa

Research Institute for Advanced Science and Technology, University of Osaka Prefecture, Sakai, Osaka, 593 Japan

Received June 17, 1994; Revised Manuscript Received August 19, 1994[⊗]

ABSTRACT: The molecular and crystal structure of the anhydrous form of chitosan, a (1→4)-linked 2-amino-2-deoxy-β-D-glucan, has been determined by combined X-ray diffraction analysis and stereochemical model refinement. Chitosan chains crystallize in an orthorhombic unit cell with dimensions a = 0.828 nm, b = 0.862 nm, and c (fiber axis) = 1.043 nm. Systematic absences are consistent with the space group $P2_12_12_1$. The unit cell comprises four glucosamine residues, giving a density of 1.52 g/cm^3. The X-ray diffraction pattern was recorded on the imaging plate, and an intensity of each reflection spot was estimated by two-dimensional measurement and subsequent background removal. Chain conformation is an extended 2-fold helix stabilized by intramolecular O3···O5 hydrogen bonds, and an O6 atom is rotated at near gt position. Two chains pass through the unit cell with an antiparallel packing arrangement. Intermolecular N2···O6 hydrogen bonds contribute to the three-dimensional stabilizing of the crystal structure. The reliability of the structure analysis is indicated by the X-ray residual R = 0.175 and R'' = 0.178 against the observed 38 *hkl*'s. Some significant similarities are observed between the anhydrous crystal structures of the present chitosan and (1→4)-β-D-mannan.

Introduction

Chitosan is a linear polymer of β-(1→4)-linked 2-amino-2-deoxy-D-glucose residues. It is readily prepared from chitin by chemical N-deacetylation and, as well as chitin, has been considered a promising material for various industrial applications. Having a regular distribution of aliphatic primary amino groups, chitosan exhibits a remarkable ability to form complexes with transition metals and salts with some acids from aqueous solution. We have reported the behavior of chitosan−metal complex formations using X-ray diffraction measurement.[1,2] It has been observed that an extended 2-fold helical conformation of the chitosan chain, originally found for tendon chitosan,[3] is retained in most of these crystals. Other X-ray diffraction studies on some chitosan salts (HF, HCl, and H_2SO_4 salts)[4] and chitosan gel[5] revealed that the chitosan backbone adopted either a left-handed (8_5) or right-handed (8_3) helix conformation. This type of helical structure was supported by the high-resolution solid-state ^{13}C NMR spectroscopy measurement of the chitosan salts, which suggested the presence of a 4-fold helical conformation of dimeric units.[6] As regards interactions between chitosan chains and metal ions in the complex crystals, two types of coordination mode have been proposed: the "pendant model"[1,7] and the "bridge model".[8,9] In the former model, a metal ion is coordinated to a single nitrogen atom like a pendant, whereas a metal ion in the latter involves four nitrogen atoms to form a "bridge" between the amino groups of intra- or interchains. A detailed crystal structure analysis shouild be undertaken by analyzing the X-ray diffraction data in order to resolve such ambiguities.

These chitosan polymorphic forms correspond to the hydrated crystals in which the water molecules may or may not be located at the crystallographically defined positions in the unit cell. Upon heating the chitosan samples in water, the crystals were converted into the anhydrous form,[10,11] which was considered to be the simplest polymorphic form containing no small molecules, such as water and metal ions. It has been also observed that chitosan samples rich in anhydrous crystals become insoluble in acidic solvents in which those involving the noncrystalline region and hydrated crystals are easily dissolved.[11] Such physical properties of chitosan, arising from the crystalline polymorph and the crystallinity, might be correlated to its chemical and biological activities. The present work was undertaken to determine the detailed crystal structure of the anhydrous form of chitosan. Given knowledge of the molecular and packing structure of the chitosan chains in the crystal, the crystal structures of more complicated as well as more interesting polymorphs of chitosan, such as the hydrate,[3] metal complexes,[2] and salts,[4] will be determined in future studies.

Experimental Section

Nomenclature. Figure 1 shows the principal parameters to describe chitosan chain conformation together with the atom labeling. The rotations of the two glycosidic linkages, Φ and Ψ, are defined by the four-atom sequences O5−C1−O1−C4′ and C1−O1−C4′−C5′, respectively. Coupled with these rotations, the glycosidic bridge angle, τ, is allowed to vary in the course of conformational refinement of the chitosan chain. The orientations of the primary hydroxymethyl groups around C5−C6 bonds (χ) is defined by the O5−C5−C6−O6 sequence. The conformation usually prefers the three staggered positions, each of which is referred to as either gauche−trans (gt), gauche−gauche (gg), or trans−gauche (tg).[12] Typical values

[⊗] Abstract published in *Advance ACS Abstracts,* November 1, 1994.

0024-9297/94/2227-7601$04.50/0

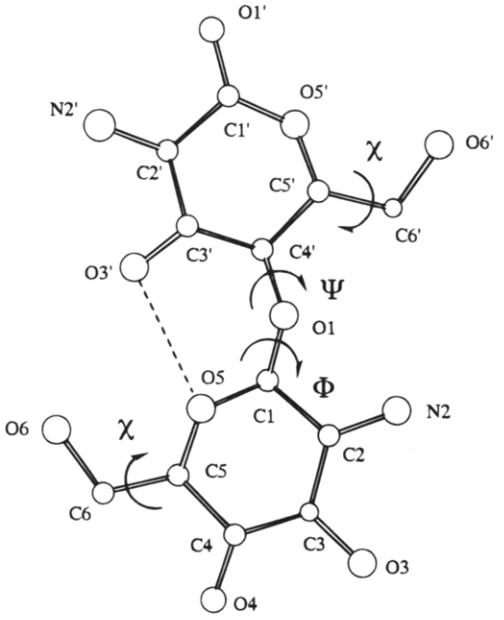

Figure 1. Atomic labeling scheme and designation of the conformational angles Φ, Ψ, and χ.

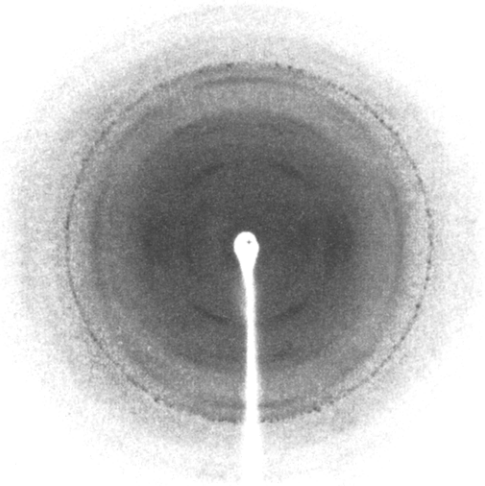

Figure 2. Fiber X-ray diffraction pattern of the chitosan anhydrous polymorphic form recorded on an imaging plate. The fiber axis is vertical, and the calibration line is the d = 0.2319 nm line of NaF.

of χ for the respective positions are gt = 60°, gg = −60°, and tg = 180°.

Materials. A tendon chitosan was prepared from the chitin crab tendon, *Chionecetes opilio* O. Fabricus, by N-deacetylation with 67% sodium hydroxide solution at 110 °C for 2 h under nitrogen atmosphere, following by treating with 1 M aqueous NaOH and subsequently washing with water.[2] This solid-state deacetylation procedure was repeated twice. It was revealed by measurement of a colloidal titration that the degree of N-acetylation of the resultant tendon chitosan was near 0%.[11] The chitosan sample showed the diffraction pattern typical of the hydrated polymorphic form when X-rayed. Its crystallinity was improved by annealing in water at 240 °C in a sealed bomb, and simultaneously, the crystalline structure was converted into the anhydrous form.

X-ray Measurement. A rotating-anode X-ray generator (RU-200, Rigaku) was operated in normal focus mode (focus 0.5 × 10 mm²) to provide a monochromatized X-ray beam (Cu Kα, λ = 0.154 18 nm, 50 kV × 140 mA). Diffraction data were recorded on the disk-shaped imaging plate (Fuji), a flexible plastic plate coated with fine photostimulative phosphor crystals, with a sample−plate distance of 75.5 mm. The diffraction pattern was read by measuring the fluorescence intensity stimulated by a focused He−Ne laser beam that scanned spirally the surface of the imaging plate. The representative diffraction pattern recorded on the imaging plate is shown in Figure 2. The measurement of X-ray diffraction data was implemented by the hardware system, DIP100S (MAC Science). The intensity values thus obtained converted into pixel data in a rectangular coordinate system. A whole area of the imaging plate (200 mm diameter) was covered with 1600 × 1600 pixels, each having a size of 125 μm². Removal of background intensity was carried out separately at each diffraction spot. The background surface was estimated by smoothly connecting the intensity levels at the four corners of a fan-shaped area that contained a single or more peaks. The intensity of each diffraction was then subjected to corrections for the Lorentz and polarization factors.

Structure Analysis and Refinement. The structure determination and refinement were carried out using the linked-atom least-squares program (LALS).[13] Models of molecular and packing structures are established by minimizing a quantity, Ω, defined by the expression

$$\Omega = \sum_m w_m(|F_{m,o}|^2 - k^2|F_{m,c}|^2) + \sum_{i,j}\epsilon_{ij} + \sum_q \lambda_q G_q \quad (1)$$

where, in the first term, $F_{m,o}$ and $F_{m,c}$ are the observed and calculated amplitudes, respectively, k is a scaling factor, and m counts all individual reflections. The weight, w_m, was equal to 1.0 for all the observed reflections, 0.5 for the unobserved ones for which $F_{m,c} > F_{m,o}$ and 0, for $F_{m,c} < F_{m,o}$. The second term evaluates the nonbonded repulsion arising between the nonbonded atoms i and j. The interaction is applied only when the distance between them falls within the standard value. The third term involves a set of coordinate constraint equations, G_q, together with their initially undefined Lagrange multipliers, λ_q. The constraints usually are used to preserve a helix continuity and a ring closeure of the residue during chain of conformational refinement.

Results

In our previous report,[10] it was suggested that the unit cell dimension of anhydrous chitosan was orthorhombic with a = 0.824 nm, b = 1.648 nm, and c (fiber axis) = 1.039 nm. The unit cell contained eight glucosamine units, corresponding to four chitosan molecular chains of a 2_1 helix conformation. The calculated crystalline density, ϱ_{calcd} = 1.52 g/cm³, was in reasonable agreement with the observed one, ϱ_{obsd} = 1.44 g/cm³. Absences of (*odd*,0,0) and (0,*odd*,0) reflections indicated the possible presence of a crystallographic 2_1 axis along both the a and b axes of the unit cell. However, most of the 22 individual reflection spots detected in the diffraction data could actually be indexed with a half-sized, two-chain unit cell about the b axis. Only the third layer's reflection (0.34 nm) with very weak intensity was unable to be assigned, and this caused doubling of the base plane dimension. The fiber diffraction data obtained in the present study exhibited similar quality in crystallinity but were higher in orientation compared with the previous data. Along with an improvement of the diffraction pattern, it was also observed that the 0.34 nm reflection on the third layer disappeared as the annealing temperature was raised to 240 °C, which as a result allowed us to adopt the two-chain unit cell. In a practical viewpoint, the structure determination can be more conveniently carried out by adopting a small unit cell. Inside the observed diffraction region, the four-chain unit cell yielded 29 unobserved *hkl*'s out of a total of 68 *hkl*'s, while halving the base plane size decreased this number to 7 out of a total of 40 *hkl*'s and consequently reduced ambiguity in the structure deter-

Table 1. Comparison of Calculated and Observed *d*-Spacings

	d-spacing (nm)			*d*-spacing (nm)	
hkl	calcd	obsd	*hkl*	calcd	obsd
110	0.5971	0.583	002	0.5215	0.520
020	0.4310	0.417	012	0.4462	0.437
200	0.4140		102	0.4413	
120	0.3823	0.372	112	0.3928	0.386
210	0.3732		022	0.3322	0.319
220	0.2986	0.288	202	0.3242	
130	0.2715	0.264	122	0.3083	0.298
310	0.2629		212	0.3035	
			222	0.2591	0.254
011	0.6644	0.650			
101	0.6485		013	0.3224	0.317
111	0.5182	0.501	103	0.3206	
121	0.3590	0.348	113	0.3005	0.298
211	0.3514		023	0.2706	0.262
221	0.2870	0.280	203	0.2662	
031	0.2770	0.262	123	0.2572	0.251
301	0.2668		213	0.2544	
			014	0.2496	0.247
			104	0.2487	
			114	0.2390	0.237

mination. Furthermore, systematic absences of (*odd*,0,0) and (0,*odd*,0) reflections were still indicated in the equatorial data indexed with the two-chain unit cell. A further refinement of the unit cell dimensions gave the new set of the parameters $a = 0.828$ nm, $b = 0.862$ nm, and $c = 1.043$ nm. A comparison between the observed and calculated *d*-spacings is listed in Table 1.

The presence of a 2_1 axis on the base plane indicates an antiparallel packing of molecular chains in the crystals, where all the chains pass through the unit cell in alternative direction. This is consistent with the fact that molecular chains of the tendon chitin has also been found to crystallize in an antiparllel chain packing fashion,[14] otherwise one must assume an entire rearrangement of the chain polarities to occur during solid-state deacetylation of the tendon chitin to provide parallel chain packing in the chitosan crystals. Possible space group that is content with antiparallel packing of the 2_1 helix chains, coupled with involvement four glucosamine residues, is either $P2_12_12_1$ or the $P2_122_1$ if the orthorhombic system is assumed. In both the cases, the molecular chains are placed on the base plane of the unit cell such that the helix axis coincides with a crystallographic 2_1 axis along the *c*, which are at (*a*/4,0) for the both space groups. Thus, the following crystal structure analysis was carried out by assuming the $P2_12_12_1$ symmetry and, for comparison, the $P2_122_1$ symmetry.

A conformational model of the chitosan chain was determined with the constraints of a 2_1 symmetry and the fiber repeat distance of 1.043 nm. The parameters changed during the structure refinement were those to describe the glycosidic linkage structure: Φ, Ψ, and τ. The sum of the nonbonded interactions that derived from the last two terms in the eq 1 was minimized. In common with other β-1→4-linked glycans of a 2_1 helical structure, the resulting conformational model involved an intramolecular hydrogen bond interaction between O3 and O5 atoms across every glycosidic linkages.

The first stage of the crystal structure analysis was to search appropriate chain-packing positions in the unit cell against the X-ray data. Chain-packing models were first determined about the chain rotational position, μ in degrees, with respect to *a* or *b* of the base plane. The helix axis was rotated from −180° to 0° in 20° increments and the crystallographic residuals *R* and *R*″ were calculated for the *hk*0 data at each position. For the $P2_12_12_1$ space group, the curves of the residuals exhibited the four minima at $\mu = -150°$, −120°, −60°, and −30°. The behavior of the crystallographic residuals at the former two minima were essentially identical to the latter two since interchanging between the *a* and *b* dimensions (an operation equivalent to rotating the helix axis 90°) caused little change in the base plane projection under the symmetry. The values of the residuals were as follows: $R = 0.08$, $R'' = 0.09$ for $\mu = -20°$ or −120°, and $R = 0.10$, $R'' = 0.11$ for $\mu = -60°$ or −150°. The curves calculated for the $P2_122_1$ space group consisted of the two distinct minima at $\mu = -120°$ ($R = 0.29$, $R'' = 0.30$) and −150° ($R = 0.35$, $R'' = 0.31$) along with the two shallow minima with unacceptable values of the residuals (>0.60). Chain translational positions, *w* in fractions, along the *c* dimension were determined in a fashion similar to the previous search of μ; *w* was stepped from −0.25 to 0.25 in 0.05 increments, and the residuals were calculated for all the *hkl* data, while the chain rotational position, μ, was fixed at either the −150° or −120° position. It was observed that variations of the residuals were relatively insensitive with respect to the stepping of *w* compared with the residual curves about μ. The minima were detected at $w = -0.25$, 0.0, and 0.15 in the X-ray residual curves calculated for the $P2_12_12_1$ space group and $w = -0.10$ and 0.15 for the $P2_122_1$ space group. Combination of every minima of μ and *w*, coupled with the three staggered positions for the O6 atom rotation, χ, provided the 27 initial packing models with the $P2_12_12_1$ space group and the 18 models with the $P2_122_1$ space group. All the initial models were subject to the chain-packing refinement against the X-ray data by minimizing the first term of the eq 1. After selecting some acceptable models, they were followed by complete structure refinement which involved the simultaneous adjustment of the chain conformational and packing parameters along with variation of the attenuation factors, *A*. In this step, the total terms of the eq 1 were optimized. Finally, intermolecular hydrogen bonds were introduced as appropriate oxygen atoms were found to be within 0.18−0.32 nm. Table 2 lists the crystallographic residuals, the contact σ that represents the stereochemical energy, the packing parameters, and the hydrogen bonds given in the final structures of the best six models with the $P2_12_12_1$ space group and the best one with the $P2_122_1$ space group. In comparison with the $P2_12_12_1$ models, it is apparent that the $P2_122_1$ model is unacceptable in terms of both the X-ray crystallography and the stereochemistry. Among the $P2_12_12_1$ models, those with the O6 gt atoms were favored by the X-ray residuals, while rotating the O6 atoms into either gg or tg position quickly raised the values. The same scheme of an intermolecular hydrogen bond (O6···N2 atoms) was detected in each of the $P2_12_12_1$ models except model 6 with the O6 tg atoms. Model 1 exhibited the lowest values of *R* and *R*″ factors together with the lowest contact σ and model 2, the second lowest ones. Differences in the X-ray residuals between the best two models are rather small but not insignificant. It, therefore, is quite reasonable to judge model 1 to be the most probable model for the crystal structure of the anhydrous chitosan. The final values for the conformational parameters of the model are $\Phi = -98°$, $\Psi = -148°$, $\tau = 116.7°$, and $\chi = 59°$. The atomic coordinates in the crystallographic repeat of this model are given in Table 3, and a comparison of the calculated and observed structure factor amplitudes is given in Table 4, showing generally good agreement. Projections of the

Table 2. Comparison of Structural Features of Models Selected for Final Structure Refinement

model	O6 position	packing parameters		X-ray residuals[c]			contact	H-bonds[g] and their lengths, nm	
		μ,[a] deg	w,[b] frac	R	R''	A[d]	σ[f]		
				$P2_12_12_1$ Space Group					
1	gt	−147	−0.122	0.175	0.178	0.114	21.1	O6···N2	0.272
2	gt	−115	0.146	0.178	0.185	0.000[e]	22.6	O6···N2	0.282
3	gt	−102	−0.111	0.198	0.207	1.078	22.4	O6···N2	0.277
4	gt	−157	0.137	0.213	0.219	0.000[e]	21.9	O6···N2	0.270
5	gg	−150	−0.130	0.234	0.245	2.594	22.0	O6···N2	0.272
6	tg	−121	0.226	0.228	0.246	0.000[e]	24.4	none	
				$P2_122_1$ Space Group					
	gt	−136	−0.114	0.335	0.405	0.000[e]	37.7	O6···N2	0.279
								O3···O3	0.272

[a] 0° position is when O4 is at (x, 0) for a helix at origin. Positive rotation is anticlockwise looking down the helix axis. [b] Fractional position of O4 atom along the c dimension. [c] $R = \Sigma||F_o| - |F_c||/\Sigma|F_o|$, $R'' = [\Sigma w||F_o| - |F_c||^2/\Sigma w|F_o|^2]^{1/2}$. [d] Attenuation factor. The value of F_c is modified by multiplication by $\exp[-A(\sin\theta/\lambda)^2]$. [e] The value of A was fixed at 0 for the models gave negative values when refined. [f] The sum of the second term of the eq 1. [g] Intermolecular bonds.

Table 3. Fractional Coordinates ($\times 10^5$) of Asymmetric Unit[a]

atom	x	y	z
C(1)	24719	4626	26232
C(2)	32700	15944	16692
C(3)	25538	14008	3329
C(4)	25806	−3789	−574
C(5)	17957	−14009	9776
C(6)	18937	−32089	6946
O(1)	33027	5465	37838
N(2)	30687	32813	20744
O(3)	34947	22621	−5735
O(4)	16971	−5467	−12159
O(5)	26232	−11470	21404
O(6)	12317	−40753	17530
H(1)	12370	8040	27576
H(2)	45316	13118	16204
H(3)	13408	18640	3204
H(4)	37941	−8005	−2075
H(5)	5588	−10394	10893
H(6a)	31177	−35909	5488
H(6b)	12393	−35054	−1939

[a] The helix axis for this residue is at (0.25, 0, w). The rest of the residues in the unit cell can be generated by the $P2_12_12_1$ symmetry operation: $(-x + 0.5, -y, z + 0.5)$, $(-x, y + 0.5, -z + 0.5)$, $(x + 0.5, -y + 0.5, z)$.

Table 4. Comparison of Calculated and Observed Structure Amplitudes

hkl	F_c	F_o	hkl	F_c	F_o
110	132.5	123.0	012, 102	58.4	86.9
020, 200	160.6	156.5	112	25.1	39.9
120, 210	129.1	120.8	022, 202	25.8	34.8
220	10.7	19.5	122, 212	38.8	44.4
130, 310	85.2	84.4	222, 302	34.0	30.7
011, 101	6.6	20.6	013, 103	27.7	52.6
111	6.7	13.4	113	44.6	55.1
021	15.7	16.3[a]	023, 203	36.3	32.5
201	13.6	15.9[a]	123, 213	51.5	41.5
121, 211	43.7	53.4	014, 104	42.6	53.0
221	44.4	40.5	114	42.0	48.7
031, 301 } 311	62.7	46.2			

[a] Unobserved reflection.

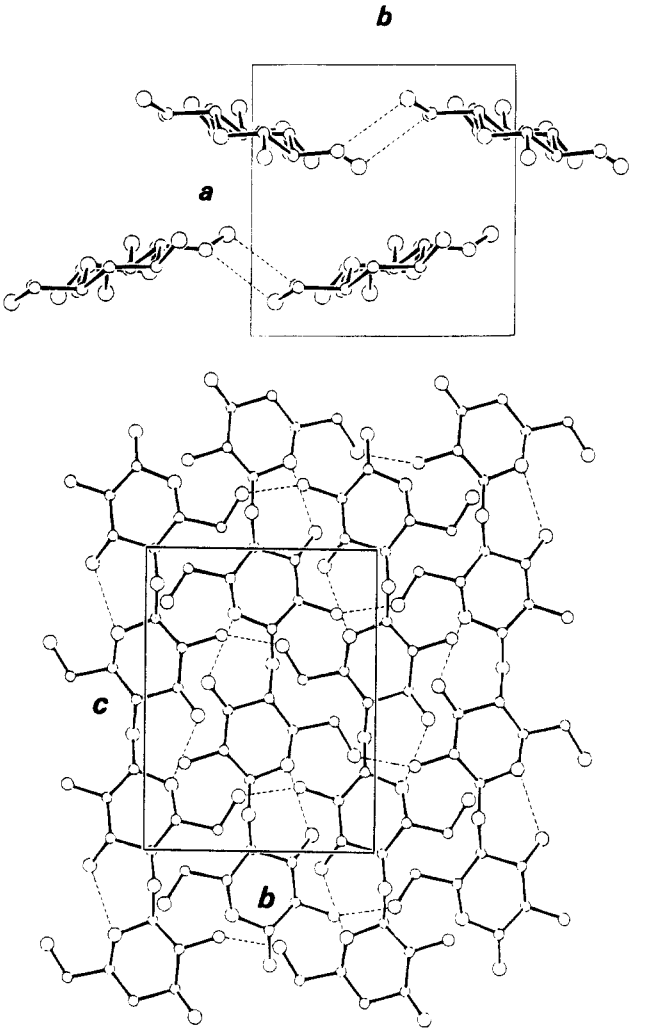

Figure 3. Projections of the crystal structure on the ab (top) and bc (bottom) base planes. All hydrogen atoms have been omitted, and hydrogen bonds are shown as dashed lines.

two base planes, complete with hydrogen bonds, are drawn in Figure 3. For a comparison, a supplementary structure analysis was carried out based on the monoclinic $P2_1$ system with the c axis unique. In the symmetry, both the chains in the unit cell were independent, which required a two-dimensional grid search for μ and w in determinations of the chain-packing positions. Combining each of the μ and w minima found on the residual surfaces, it turned out that the resulting best packing structure was virtually consistent with model 1 of the $P2_12_12_1$ space group. This rejected the possibility of $P2_1$ symmetry and, simultaneously, ensured the suitability of model 1.

Conclusion

The crystal structure of the chitosan polymorph was first reported by Sakurai et al.[15] The unit cell parameters proposed for the polymorph were $a = 0.867$ nm, $b = 0.892$ nm, c (fiber axis) = 1.024 nm, and $\gamma = 92.6°$, and no symmetry element was suggested. In spite of a rather slight difference in the base plane dimension from that proposed for the anhydrous form of chitosan the chain-packing structure was quite different; two

independent chains in antiparallel polarity were placed on either (0,0) or (0,*b*/2) of the base plane such that their pyranose planes were nearly parallel to the (010) reflection plane. Recently, Cartier et al. reported the electron diffraction data of the chitosan single crystals.[16] The unit cell parameters derived from the data were a = 0.807 nm, b = 0.844 nm, and c (fiber axis) = 1.034 nm, and the $P2_12_12_1$ symmetry was also suggested from systematic absences of (*odd*,0,0) and (0,*odd*,0) reflections. Clearly, these results suggested that the polymorphic form obtained from the single crystals corresponded to the anhydrous chitosan in the present study. Although the list of structural parameters and atom coordinates were not given in the report, the projections of the proposed crystal structure appeared to be similar to our result.[17]

Comparing with the regenerated crystal structures observed for the other polysaccharides with a 2_1 helical conformation, it is suggested that the resulting structure of anhydrous chitosan is similar in some significant respects to that of mannan I, the anhydrous polymorph of (1→4)-β-D-mannan.[18] Either the chitosan or mannan chain, having all O6 atoms in the gt position, crystallizes into the two-chain, orthorhombic unit cell with the $P2_12_12_1$ space group. The packing parameters of mannan I, $\mu = -151°$ and $w = -0.0862$ with respect to the O4 atom, are close to those of the chitosan anhydrous structure (See Table 1). More importantly, both crystal structures contain a single intermolecular hydrogen bond per residue, although atoms involving the bond are different (O2···O5 in mannan I). The bonding sequences in the mannan I crystal structure construct the sheets of the molecular chains parallel to the (100), (010), or (110) reflection planes such as, combined with the intramolecular hydrogen bond along the c axis, to establish the three-dimensional hydrogen bond stabilized network. In the chitosan anhydrous structure, the sequences of intermolecular hydrogen bond develop only along the (100) reflection plane to form the one-dimensional chain sheet. It, therefore, is likely that hydration and coordination of metal ions occur between the sheets in the corresponding chitosan polymorphs. It should be noted that the regenerated, anhydrous crystals obtained from the two typical glucans of the 2_1 helix, cellulose and (1→3)-α-D-glucan, exhibit a more intensive scheme of intermolecular hydrogen bonds of 2.5 bonds per glucose residue.[19,20] In these glucan crystal structures, every hydroxyl oxygen participates in either intra- or intermolecular hydrogen bonds. As for the mannan and chitosan, in comparison with the glucans, an axial hydroxyl or an amino group present on C2 of each residue appears to disturb effective formations of hydrogen bonds between the molecular chains with the 2_1 symmetry on anhydrous crystallization. When exposed to an aqueous solvent, the chitosan and mannan chains may preferentially crystallize in hydrated forms where the intermolecular hydrogen bond dominantly occurs between sugar residues and water molecules to complement the bonding network. The water molecules, being accessible to the surface of the sugar residues, readily develop hydrogen bond interactions with the molecular chains, and as a result, they intervene between chains or chain sheets through the bonds in the crystal structures. Chitosan crystals have been first observed as hydrated polymorph after either solid-state deacetylation of tendon, naturally oriented chitin fiber,[2] or orientation of a regenerated film.[10] A hydrated form of mannan, designated as mannan II, has also been found in the crystalline microfibrils of the cell walls of the green algae along with the mannan I crystals.[21] The detailed crystal structure analysis of mannan II indicated that intermolecular hydrogen bonds exclusively occur between mannan chains and water molecules, the latter residing at the particular crystallographic positions.[22] It would be of interest to determine the hydrated crystal structure of chitosan and to reveal, in particular, the hydration and hydrogen bonding scheme. A further comparison can thus be made between the crystal structures of the chitosan hydrate and mannan II. This work is underway.

References and Notes

(1) Ogawa, K.; Oka, K.; Miyanishi, T.; Hirano, S. In *Chitin, Chitosan and Related Enzymes*; Zikakis, J. P., Ed.; Academic Press: Orlando, FL, 1984; pp 327–345.
(2) Ogawa, K.; Oka, K.; Yui, T. *Chem. Mater.* **1993**, *5*, 726.
(3) Clark, G. L.; Smith, A. F. *J. Phys. Chem.* **1937**, *40*, 863.
(4) Ogawa, K.; Inukai, S. *Carbohydr. Res.* **1987**, *160*, 425.
(5) Cairns, P.; Miles, M. J.; Morris, V. J.; Ridout, M. J.; Brownsey, G. J.; Winter, T. W. *Carbohydr. Res.* **1992**, *235*, 23.
(6) Saitô, H.; Tabeta, R.; Ogawa, K. *Macromolecules* **1987**, *20*, 2424.
(7) Domard, A. *Int. J. Biol. Macromol.* **1987**, *9*, 88.
(8) Yaku, F.; Muraki, E.; Tsuchiya, K.; Shibata, Y.; Koshijima, T. *Cellul. Chem. Technol.* **1977**, *11*, 421.
(9) Schlick, S. *Macromolecules* **1986**, *19*, 192.
(10) Ogawa, K.; Hirano, S.; Miyanishi, T.; Yui, T.; Watanabe, T. *Macromolecules* **1984**, *17*, 973.
(11) Ogawa, K. *Agric. Biol. Chem.* **1991**, *55*, 2375.
(12) Marchessault, R. H.; Pérez, S. *Biopolymers* **1979**, *18*, 2369.
(13) Smith, P. J.; Arnott, S. *Acta Crystallogr.* **1972**, *A34*, 3.
(14) Minke, R.; Blackwell, J. *J. Mol. Biol.* **1978**, *120*, 167.
(15) Sakurai, K.; Shibano, T.; Kimura, K.; Takahashi, T. *Sen-i Gakkaishi* **1985**, *41*, 85.
(16) Cartier, N.; Mazeau, K.; Chanzy, H. In *Advances in Chitin and Chitosan*; Brine, et al., Eds.; Elsevier Applied Science: London, 1992; p 155.
(17) Comparing between the *ab* projections of the two crystal structure, one finds a 90° difference in chain rotational position, μ. This, however, should not cause any significant change in the three-dimensional structure due to a near quadrate feature of the base plane.
(18) Chanzy, H.; Pérez, S.; Miller, D. P.; Paradossi, G.; Winter, T. W. *Macromolecules* **1987**, *20*, 240.
(19) Stipanovic, A. J.; Sarko, A. *Macromolecules* **1976**, *9*, 851.
(20) Ogawa, K.; Okamura, K.; Sarko, A. *Int. J. Biol. Macromol.* **1981**, *3*, 31.
(21) Frei, E.; Preston, R. D. *Proc. R. Soc. London* **1968**, *B169*, 127.
(22) Yui, T.; Ogawa, K.; Sarko, A. *Carbohydr. Res.* **1992**, *229*, 41.